ARCHIVES OF THE TURKISH SOCIETY OF CARDIOLOGY

Official journal of the TURKISH SOCIETY OF CARDIOLOGY

Coexistence of Large Atrial Septal Defect with Arrhythmogenic Right Ventricular Cardiomyopathy

Büyük Atriyal Septal Defektin Aritmojenik Sağ Ventrikül Kardiyomiyopatisi ile Birlikte Bulunması

CASE IMAGE
OLGU GÖRÜNTÜSÜ

A 60-year-old woman with exertional dyspnea and palpitations was referred to our echocardiography clinic for further evaluation. Her past medical history and physical examination findings were unremarkable. Electrocardiography revealed low voltage with a QS pattern in the inferior and precordial leads, T-wave inversion in V_1–V_5, and no other significant ST-T changes (Figure 1). Transthoracic and transesophageal echocardiography showed a normal left ventricular (LV) size with mild systolic dysfunction (ejection fraction, 50%), severe right ventricular (RV) enlargement with moderately severe systolic dysfunction, RV free-wall akinesia with aneurysm formation, a dilated right ventricular outflow tract (RVOT; 18 mm/m^2), biatrial enlargement, severe tricuspid regurgitation with an estimated systolic pulmonary artery pressure of 34 mmHg, moderate pericardial effusion, and a large secundum-type atrial septal defect (ASD; 21 × 13 mm) with a significant left-to-right shunt on color Doppler study, suitable for device closure (Figure 2, Videos 1 and 2). Given the significant RVOT dilation, RV free-wall hypokinesia, significant RV dysfunction, and T-wave inversion in precordial leads, the patient underwent cardiac magnetic resonance imaging to evaluate arrhythmogenic RV cardiomyopathy. The imaging confirmed the echocardiography findings and demonstrated an RV end-diastolic volume of 139 mL/m^2, an RV ejection fraction of 39%, multiple aneurysm formations, and dyskinetic regions in the RV free wall and RVOT. The imaging also revealed multiple areas of patchy transmural late gadolinium enhancement in the RV free wall and apex, at the RV insertion points to the LV, and subepicardial and mid-wall late gadolinium enhancement in the basal interventricular septum (Figure 3, Videos 3 and 4). These findings confirmed the diagnosis of arrhythmogenic right ventricular cardiomyopathy (ARVC) with biventricular involvement and RV predominance. Ultimately, the ASD was closed using an Amplatzer ASD device occluder.

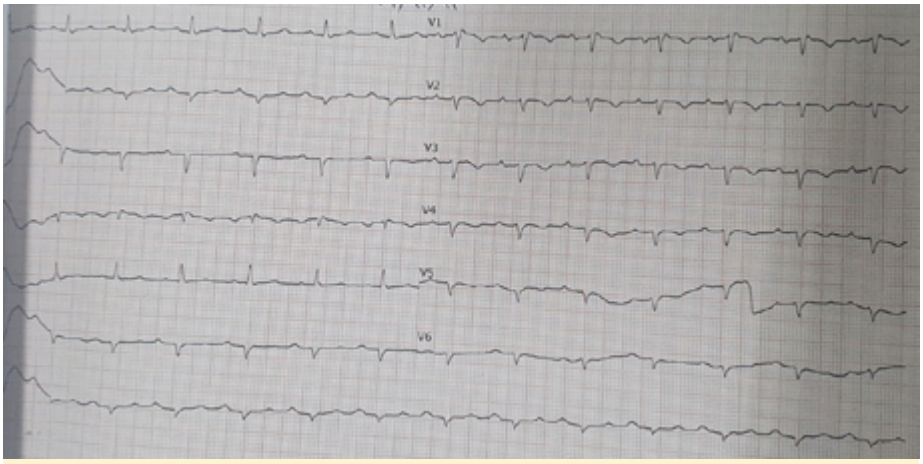

Figure 1. Electrocardiography demonstrates low-voltage QRS, a QS pattern in inferior and precordial leads, T-wave inversion in V_1–V_5, and no other significant ST-T changes.

Samira Shirzad
Sahar Asl Fallah
Ali Mohammad Hajizeinali
Ali Hosseinsabet

Department of Cardiology, Tehran Heart Center, School of Medicine, Tehran University of Medical Sciences, Tehran, Iran

Corresponding author:
Ali Hosseinsabet
✉ ali_hosseinsabet@yahoo.com

Received: July 23, 2024
Accepted: September 28, 2024

Cite this article as: Shirzad S, Asl Fallah S, Hajizeinali AM, Hosseinsabet A. Coexistence of Large Atrial Septal Defect with Arrhythmogenic Right Ventricular Cardiomyopathy. *Turk Kardiyol Dern Ars.* 2025;53(3):215–216.

DOI: 10.5543/tkda.2024.81889

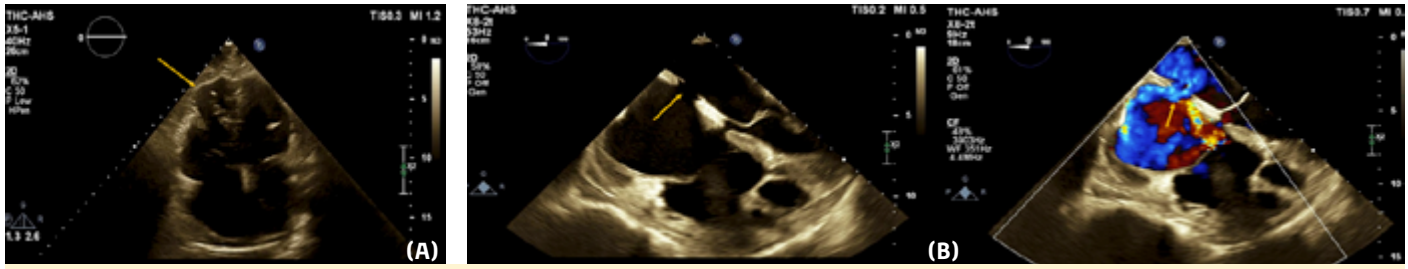

Figure 2. (A) Transthoracic echocardiography shows right ventricular enlargement with aneurysm formation in the right ventricular free wall in the apical four-chamber view. (B) Transesophageal echocardiography demonstrates a secundum-type atrial septal defect in the mid-esophageal four-chamber view.

To our knowledge, the coexistence of ASD and ARVC is rare, with fewer than 10 reported cases in the literature. The imaging characteristics of these two conditions can overlap; however, any suspicious clinical, electrocardiographic, or imaging findings in patients with ASD should alert cardiologists to the potential presence of ARVC, both before and after ASD closure. These indicators, as observed in the present patient, can be particularly helpful in adult patients.

Informed Consent: The informed consent was obtained.

Peer-review: Internally peer-reviewed.

Author Contributions: Concept – S.S., S.A.F., A.M.H., A.H.; Design – S.S., S.A.F., A.M.H., A.H.; Supervision – S.S., S.A.F., A.M.H., A.H.; Resource – S.S., S.A.F., A.M.H., A.H.; Materials – S.S., S.A.F., A.M.H., A.H.; Data Collection and/or Processing – S.S., S.A.F., A.M.H., A.H.; Analysis and/or Interpretation – S.S., S.A.F., A.M.H., A.H.; Literature Review – S.S., S.A.F., A.M.H., A.H.; Writing – S.S., S.A.F., A.M.H., A.H.; Critical Review – S.S., S.A.F., A.M.H., A.H.

Conflict of Interest: The authors have no conflicts of interest to declare.

Funding: The authors declared that this study received no financial support.

Video 1. Transthoracic echocardiography demonstrates a dilated right ventricular outflow tract, right ventricular hypokinesia, a dilated right ventricle with free-wall akinesia, and aneurysm formation before and after atrial septal defect device closure.

Video 2. Transesophageal echocardiography presents the atrial septal defect and the dilated right ventricle with systolic dysfunction.

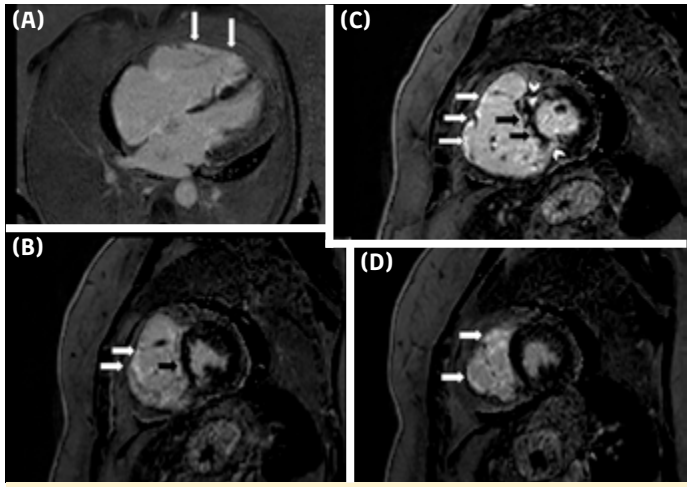

Figure 3. Phase-sensitive inversion recovery sequence in four-chamber (A), short-axis at base (B), mid (C), and apical (D) short-axis views shows patchy late gadolinium enhancement in the right ventricular wall (white arrows), right ventricular insertion points (white arrowheads), and subepicardial late gadolinium enhancement in the left ventricular septum (black arrows).

Video 3. Cine steady-state free precession sequence in the four-chamber view shows right ventricular dilation, moderate dysfunction, and microaneurysm formation near the right ventricular apex.

Video 4. Cine steady-state free precession sequence in right ventricular inlet/outlet views shows multiple microaneurysm formations in the right ventricular inlet and outlet walls.